Analyst



PAPER



Cite this: Analyst, 2022, 147, 5462

Ultrasensitive detection of acephate based on carbon quantum dot-mediated fluorescence inner filter effects†

Haiqin Li, a Rong Deng, Da Hamed Tavakoli, b Xiaochun Li and XiuJun Li b *b

Acephate is an organophosphorus pesticide (OP) that is widely used to control insects in agricultural fields such as in vegetables and fruits. Toxic OPs can enter human and animal bodies and eventually lead to chronic or acute poisoning. However, traditional enzyme inhibition and colorimetric methods for OPs detection usually require complicated detection procedures and prolonged time and have low detection sensitivity. High-sensitivity monitoring of trace levels of acephate residues is of great significance to food safety and human health. Here, we developed a simple method for ultrasensitive quantitative detection of acephate based on the carbon quantum dot (CQD)-mediated fluorescence inner filter effect (IFE). In this method, the fluorescence from CQDs at 460 nm is quenched by 2,3-diaminophenazine (DAP) and the resulting fluorescence from DAP at 558 nm is through an IFE mechanism between CQDs and DAP, producing ratiometric responses. The ratiometric signal I_{558}/I_{460} was found to exhibit a linear relationship with the concentration of acephate. The detection limit of this method was 0.052 ppb, which is far lower than the standards for acephate from China and EU in food safety administration. The ratiometric fluorescence sensor was further validated by testing spiked samples of tap water and pear, indicating its great potential for sensitive detection of trace OPs in complex matrixes of real samples.

Received 21st September 2022, Accepted 26th October 2022 DOI: 10.1039/d2an01552h

rsc.li/analvst

1. Introduction

In recent decades, organophosphorus pesticides (OPs) such as acephate have been widely used in the prevention, control and elimination of plant diseases and insect pests on vegetables and fruits. However, except approximately 2.5% of the pesticides used for pest control, the remaining 97.5% is left in the soil, atmosphere, and water resources. This eventually inhibits the activity of cholinesterase when it enters the human body directly or indirectly through bioconcentration, direct human contact, and eating, resulting in a large accumulation of the neurotransmitter acetylcholine (ATCh). As a consequence, the accumulated ATCh blocks nerve conduction, poisoning the central nervous system and harming human health. This has become an increasing issue as the abuse of pesticides is currently a global concern. Therefore, the

A variety of well-developed technologies have been applied for the detection of OPs mainly including gas chromatography (GC), 8,9 high-performance liquid chromatography (HPLC), 10 and capillary electrophoresis. 11 Although they possess obvious advantages in terms of detection accuracy, high throughput, and reproducibility, these methods require sophisticated and expensive detection instruments, and time-consuming and professional operations. Therefore, more rapid and low-cost biosensors have been explored for the quantitation of pesticides, mainly including enzyme-linked immunosorbent assays, 12 electrochemical methods, 13,14 enzyme inhibition combined with colorimetric analysis methods, 15-18 and surface enhanced Raman scattering. 19,20 However, these methods still have shortcomings such as low sensitivity, requirements of high-affinity antibodies, and false-positive results (low specificity). Thus, there is an urgent need to develop new highly sensitive methods for the detection of OPs.

Due to the high sensitivity, fast response, and high signalto-noise ratios of fluorescence, ^{21,22} fluorescence-based biochemical sensors have been developed for OPs quantitation,

maximum allowable limits of different OPs have been set by regulatory agencies. For instance, the maximum allowable limit of acephate in food is 0.02 ppm.⁷ Hence, it is very important to accurately detect and quantify trace levels of pesticides in food and the environment.

^aInstitute of Biomedical Precision Testing and Instrumentation, College of Biomedical Engineering, Taiyuan University of Technology, Jinzhong 030600, P.R. China. E-mail: lixiaochun@tyut.edu.cn

^bDepartment of Chemistry and Biochemistry, Forensic Science, & Environmental Science & Engineering, University of Texas at El Paso, 500 W University Ave, El Paso, Texas 79968, USA. E-mail: xli4@utep.edu

[†] Electronic supplementary information (ESI) available. See DOI: https://doi.org/10.1039/d2an01552h

including silicon quantum dots (SiQDs),²³ CdTe/ZnCdSe quantum dots,24 organic fluorescent dyes25 and aggregationinduced emission molecules (AIE).²⁶ However, most of these metal-based quantum dots or organic fluorescent molecules usually have poor water solubility, long preparation time, and toxicity, which lead to limited applications in food safety surveillance. Conversely, as a new type of carbon-based nanomaterial, carbon quantum dots (CODs) possess many advantages such as tunable fluorescence emission dependent on size and excitation wavelength, ease of preparation, 27 high stability, better water solubility, non-toxicity and excellent biocompatibility.²⁸ Furthermore, compared with other fluorescence quenching mechanisms such as static quenching, dynamic quenching, photoinduced electron transfer (PET), and Förster resonance energy transfer (FRET), the fluorescence inner filter effect (IFE) can be readily used for CQD-based fluorescence sensors without complicated functional modification of CQDs and any electron or energy transfer processes.²⁹ Similar to FRET, the IFE also depends on the spectral overlap between a fluorophore and an absorber. However, there is no distance requirement between the energy donor and the absorber in the IFE. 30 The IFE occurs when the absorption spectrum of the quencher in the detection system overlaps the excitation or emission spectrum of CQDs.31 Therefore, the combination of CQDs and the fluorescence IFE mechanism will provide a new, facile and low-cost strategy for sensitive fluorescence detection of OPs.

Herein, we designed a sensitive acephate detection method based on enzyme inhibition and the CQD-mediated IFE effect. A detection strategy with fluorescence ratiometric response characteristics was developed using OPD and CQDs as indicators. In the presence of acephate, acephate acts as an inhibitor of AChE and blocks the production of thiocholine, which prevents the formation of Ag⁺ metal-polymers, and further triggers the oxidation of OPD to produce yellow 2,3-diaminophenazine (DAP) with fluorescence emission at 558 nm. The fluorescence intensity of CQDs (460 nm) is quenched by the IFE process due to the overlapped spectra of DAP, producing a typical ratiometric response. This method is simple and sensitive, and has achieved a limit of detection of 0.052 ppb, three orders of magnitude lower than the maximum allowable limit of acephate. This fluorescence method based on the CQDmediated IEF has been further validated by testing tap water and pear samples spiked with acephate, indicating its high potential for facile and sensitive detection of OPs.

2. Experimental section

2.1 Reagents and instruments

CQDs (size 4.5 nm, 50 mg mL $^{-1}$) were purchased from Xingzi New Material Development Co., Ltd. Acephate and acetamiprid (100 µg mL $^{-1}$ in methanol) were procured from Beijing Tanmo Quality Inspection Technology Co., Ltd. Thiram was purchased from Shanghai Titan Technology Co., Ltd. SDM and CaCl $_2$ were provided by Shanghai Aladdin Biochemical Technology

Co., Ltd. OPD was obtained from Xinfan Biological Technology Co., Ltd. Silver nitrate was purchased from Kermel Chemical Reagent Co., Ltd (Tianjin, China). A pesticide rapid detection kit was purchased from Dayuan Oasis Food Safety Co., Ltd (Guangzhou, China), which included the substrate (acetylcholine, ATCh), the hydrolytic catalyst (acetylcholinesterase, AChE), and phosphate buffer (pH = 8.0, used for eluting methyl parathion residues in fruits and vegetables).

The UV-vis absorbance spectra were measured using a UV-3100 spectrometer (Shanghai Mapada Instrument Co., Ltd). The FL emission and excitation spectra were obtained using a fluorescence spectrometer FluroMax-4 (HORIBA Scientific). Deionized water (specific resistivity 18.2 M Ω cm) produced with a Barnstead EasyPure UV/UF compact water system (Dubuque, IA) was used to prepare all buffers/solutions throughout the experiments. Ag⁺-thiocholine complexes and CQDs were characterized by XPS (Fig. S1†) and high-resolution TEM (Fig. S2†), respectively.

2.2 Optimization of Ag⁺ concentration

A series of Ag^+ solutions with different concentrations of 0, 17, 34, 68, 85, 170, 340, 510, 680, 850, 1020, 1190, 1360, 1530, and 1700 µmol L^{-1} were prepared in brown centrifuge tubes. Afterward, 250 µg m L^{-1} CQDs and 25 mmol L^{-1} OPD were added to these centrifuge tubes. After mixing, the reaction solution was left in a brown centrifuge tube for 5 minutes. Subsequently, the reacted solution was transferred to a micro quartz cuvette (300 µL each) for fluorescence emission spectroscopy measurement with an excitation wavelength of 360 nm. Finally, the emission peaks of CQDs at 460 nm and DAP at 558 nm were recorded to calculate the ratiometric response I_{558}/I_{460} .

2.3 Quantitative detection of acephate

A series of acephate solutions with different concentrations were first prepared to establish calibration curves. 1 μ L of AChE was mixed with 25 μ L of each acephate solution with different concentration and were left to react at room temperature for 25 minutes. Subsequently, 1 μ L of ATCh was added and incubated in the dark at 37 °C for 15 minutes. After these incubation processes, a solution with 95 μ L of 700 μ mol L⁻¹ Ag⁺, 283 μ L of 250 μ g mL⁻¹ CQDs and 95 μ L of 25 mmol L⁻¹ OPD was added and mixed in the reaction system. After 5 minutes of reaction in each of the brown centrifuge tubes at 37 °C, the fluorescence spectra were measured under 360 nm excitation. The fluorescence signals of the CQDs at 460 nm (I_{460}) and DAP at 558 nm (I_{558}) were recorded, and the ratiometric fluorescence signal I_{558}/I_{460} was used for quantitative analysis of acephate.

2.4 Real sample preparation

Different concentrations of standard acephate (400, 200, 100, and 40 ng $\rm mL^{-1}$) were mixed with tap water from our laboratory faucets in a volume ratio of 1:1, and the final spiked concentrations were 200, 100, 50, and 20 ng $\rm mL^{-1}$.

Paper Analyst

Fresh pears were purchased from a local supermarket and were washed thoroughly with ultrapure water. The pears were cut into five pieces. The samples (1.0 g each) were spiked with 0, 2000, 4000, 6000 and 8000 ng mL⁻¹ acephate. The spiked samples were mixed with 5 mL of acetonitrile, extracted ultrasonically for 10 min, and centrifuged for 10 min at 4000 rpm. 3.5 mL of the supernatant was extracted and filtered through anhydrous sodium sulfate, and the volume was adjusted to 5 mL for detection. The final spiked concentrations were 0, 23.33, 46.67, 70.00 and 93.33 ng mL⁻¹.

3. Results and discussion

3.1 Principle of the acephate detection system

The principle of the ratiometric FL protocol is illustrated in Fig. 1, in which the enzyme inhibition method is combined with the IFE to achieve sensitive quantitation of acephate. When there is no acephate, AChE hydrolyzes ATCh to generate thiocholine,³² which combines with Ag⁺ to form metal-polymers.³³ Hence, the fluorescence intensity of the reaction

mainly comes from the emission of CQDs at 460 nm. However, in the presence of acephate, which acts as an inhibitor of AChE, acephate will prevent the hydrolysis of ATCh and inhibits thiocholine production, thereby preventing the formation of metal-polymers formed by thiocholine and Ag^+ . Furthermore, the oxidation of OPD by Ag^+ is triggered and yellow DAP is generated, which emits fluorescence at 558 nm (excitation 360 nm) and quenches the fluorescence intensity of CQDs through the IFE. By establishing the relationship curve between the concentration of acephate and I_{558}/I_{460} , the quantitative detection of acephate can be realized.

In this work, the IFE between CQDs and DAP is key to the high-sensitivity quantification of acephate. Fig. 2(a) shows the absorption spectra of OPD and DAP and the emission spectra of CQDs. It can be seen that there are large overlaps between the emission spectrum of CQDs and the absorption spectrum of DAP, which contributes to the generation of the IFE mechanism, and provides the feasibility of establishing the ratiometric responses of the fluorescence intensity of DAP and CQDs.

After establishing the aforementioned acephate detection system, the feasibility of the ratiometric system for sensitive

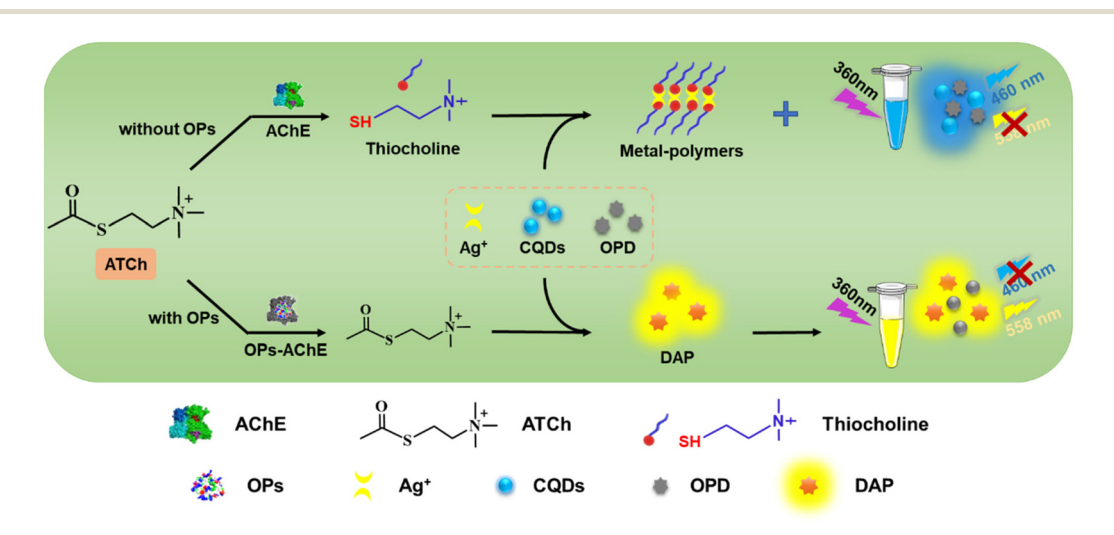


Fig. 1 Schematic illustration of the principle of sensitive and quantitative detection of acephate based on the CQD-mediated IFE.

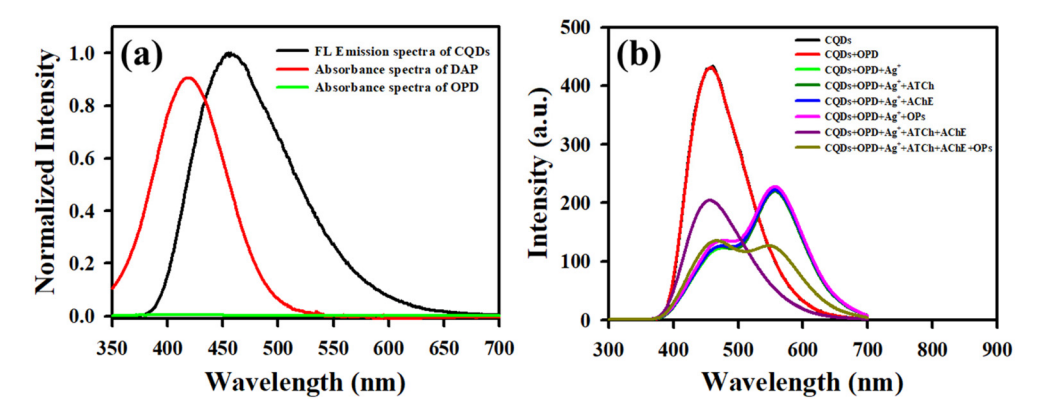


Fig. 2 (a) UV-vis absorbance spectra of OPD and DAP, and the fluorescence spectra of CQDs. (b) Feasibility test of the ratiometric strategy.

detection of acephate was evaluated by testing OPD, Ag⁺, ATCh, AChE, and OPs, respectively. As shown in Fig. 2(b), when there were only CQDs and colorless OPDs in the system, only the characteristic emission peaks (black and red curve) of CQDs are displayed. Once Ag+ was further added to the above system, the colorless OPD generated DAP due to the oxidation of Ag+, which effectively quenched the fluorescence intensity of CQDs through the IFE mechanism, resulting in the appearance of double fluorescence peaks (green curve). When ATCh, AChE, or OPs were added to the system separately, because ATCh, AChE or OPs alone did not have an effect on the system, the peaks remained the same, including the characteristic peaks of CQDs and DAP. When ATCh and AChE were added at the same time, the hydrolysate of ATCh preferentially produced metal-polymers with Ag⁺, and the oxidation of OPD was inhibited (purple line), leading to only one peak from CQDs. On the other hand, when an OP was added to the detection system, it irreversibly prevented the catalytic activity of AChE, leading to the inhibition of ATCh hydrolysis. Therefore, the dual effects from the CQD-emitted fluorescence and the inhibitory effect from DAP (i.e., the IFE), which was correlated to the concentration of the OPs, produce the ratiometric FL signal for quantitative detection of OPs, and the yellow line further confirmed its feasibility.

3.2 Influences of Ag⁺ and OPD on the fluorescence of CQDs

To verify that the quenching of the fluorescence intensity of CQDs in the detection system is only caused by the change of Ag^+ concentrations due to the change of acephate concentrations, and OPD or Ag^+ itself will not affect the fluorescence intensity of CQDs, we separately studied the effects of adding different concentrations of Ag^+ and different concentrations of OPD on the fluorescence intensity of CQDs. 250 $\mu g \ mL^{-1}$ CQDs were mixed with Ag^+ solutions at different concentrations (0, 100, 200, 300, 400, 500 $\mu mol \ L^{-1}$) at a volume ratio of 1:1. Under excitation with 360 nm light, the measured fluorescence intensities of CQDs with different concentrations of Ag^+ at 460 nm are shown in Fig. 3(a). With the addition of

different concentrations of Ag⁺, the fluorescence intensity of CQDs remained almost unchanged.

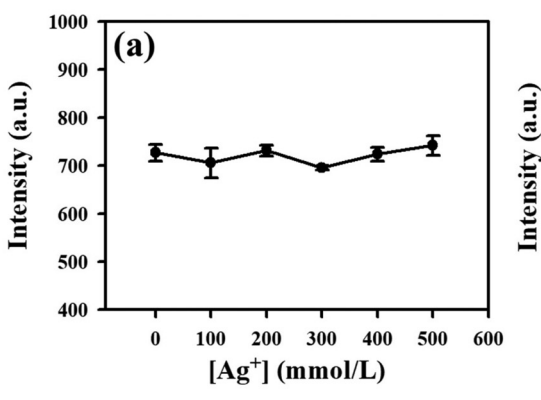
In addition, we explored the influence of different concentrations of OPD on the fluorescence intensity of CQDs. After mixing 250 $\mu g\ mL^{-1}$ CQDs with different concentrations (0, 2.0, 4.0, 6.0, 8.0, 10.0 mmol $L^{-1})$ of OPD (volume ratio 1:1), the fluorescence intensity was measured and is shown in Fig. 3(b). With the addition of different concentrations of OPD, the fluorescence intensity of CQDs also remained virtually unchanged. Thus, the above experimental results confirmed that the addition of Ag^+ or OPD alone does not cause the fluorescence quenching of CQDs.

3.3 Optimization of Ag⁺ concentration

To confirm the IFE effect between CQDs and DAP, different Ag^+ concentrations (0–1000 µmol L^{-1}) were added to the system and were left to react for 5 minutes. We can see from Fig. 4(a) that as the Ag^+ concentration increased, the fluorescence intensity of CQDs at 460 nm gradually decreased, while the emission intensity of DAP at 558 nm gradually increased, which further verified the IFE effect between CQDs and DAP. Fig. 4(b) shows the trend of the fluorescence intensity at 558 nm with the change of the Ag^+ concentration. The fluorescence at 558 nm from DAP gradually increased with the increase of the Ag^+ concentration. When the Ag^+ concentration was 700 µmol L^{-1} , DAP's fluorescence enhancement at 558 nm reached saturation. Therefore, the final concentration of Ag^+ was chosen to be 700 µmol L^{-1} for the optimal detection of acephate in the subsequent experiments.

3.4 Quantitative detection of acephate based on enzyme inhibition combined with IFE effects

After condition optimization, we tested various concentrations of acephate using the biosensor based on enzyme inhibition and the CQD-mediated fluorescence inner filter effect. Fig. 5(a) shows the fluorescence spectra measured using a fluorescence spectrometer under 360 nm excitation, with different concentrations of acephate ranging from 0 to 100 ng mL⁻¹. It can be seen that with the increase in the concentration of acephate,



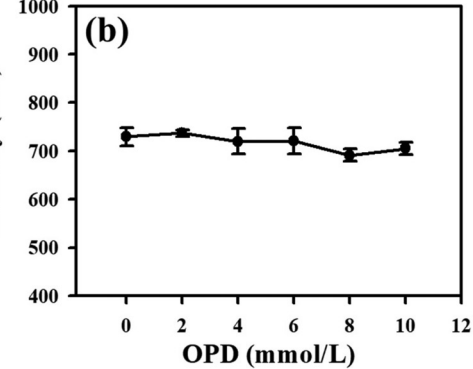


Fig. 3 The effect of Ag⁺ (a) and OPD (b) on CQDs fluorescence intensity.

Paper Analyst

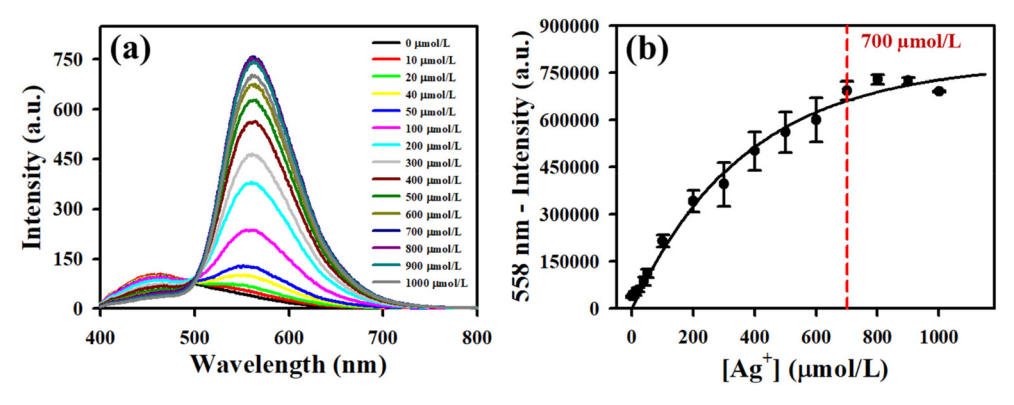


Fig. 4 Optimization of the concentration of Ag^+ . (a) Fluorescence spectra obtained at different concentrations of Ag^+ . (b) The fluorescence intensity at 558 nm with the change of Ag^+ concentration. When the concentration of Ag^+ was 700 μ mol L^{-1} , the fluorescence enhancement of the DAP was saturated.

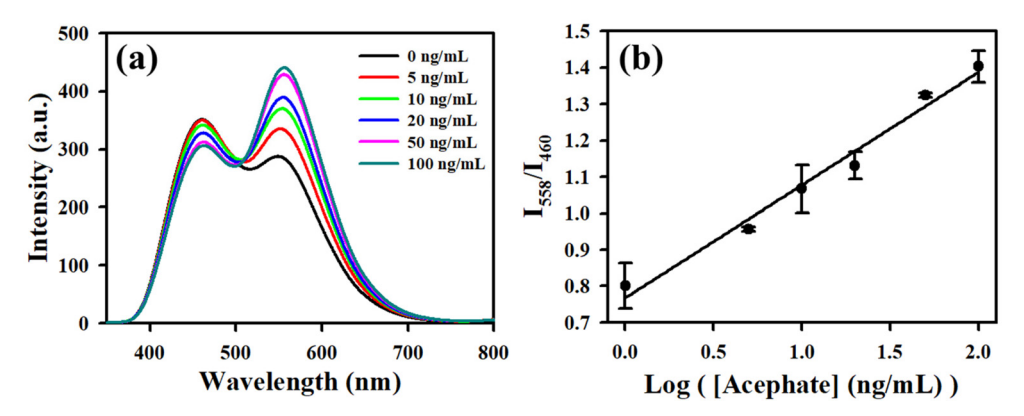


Fig. 5 (a) Fluorescence spectra of acephate at different concentrations (0, 5, 10, 20, 50 and 100 ng mL⁻¹) measured using the biosensor based on enzyme inhibition combined with the IFE effects. (b) Linear plot of ratiometric response I_{558}/I_{460} versus the logarithm of the concentration of acephate.

the fluorescence intensity (460 nm) of CQDs gradually weakened, while the fluorescence intensity (558 nm) of DAP gradually increased. A good linear relationship (R^2 = 0.981) between the ratiometric response (I_{558}/I_{460}) and the logarithm of the concentration of acephate was obtained over the range from 0 to 100 ng mL⁻¹ as shown in Fig. 5(b). The regression equation is $y = 0.3098(\pm 0.0225)\log_{10}X + 0.7677(\pm 0.0320)$, where X is the concentration of acephate and y is the fluorescence ratiometric signal I_{558}/I_{460} . According to the 3σ principle (signal-tonoise ratio of 3), the detection limit of this detection method was calculated to be 0.052 ppb. Compared with other OPs

detection methods, as listed in Table 1, our detection system has a much lower detection limit and wider linear range (Table 1). Our LOD is at least 40 times lower than (compared to 2 ppb) those of other methods.

3.5 Acephate detection in real samples

From the perspective of real world applications, it is crucial to evaluate the method by testing acephate residues in food products and environmental samples. In this work, the application of this detection method was demonstrated by testing tap water and pear samples spiked with acephate.

Table 1 Comparison with other detection methods for OPs

Sensing method	Linear range	LOD	Ref.
Colorimetric enzymatic inhibition	10-500 nM	10 nM	17
Electrochemical	2–20 ppb	2 ppb	13
Fluorescence	0.015–1.5 mM	24.7 ng mL^{-1}	26
Surface-enhanced Raman	$0.5-100.2 \text{ mg L}^{-1}$	$0.5~{ m mg}~{ m L}^{-1}$	20
GC-MS/MS	16–100 ppb	5 ppb	34
IFE fluorescence	0–100 ng mL ⁻¹	0.052 ppb	This work

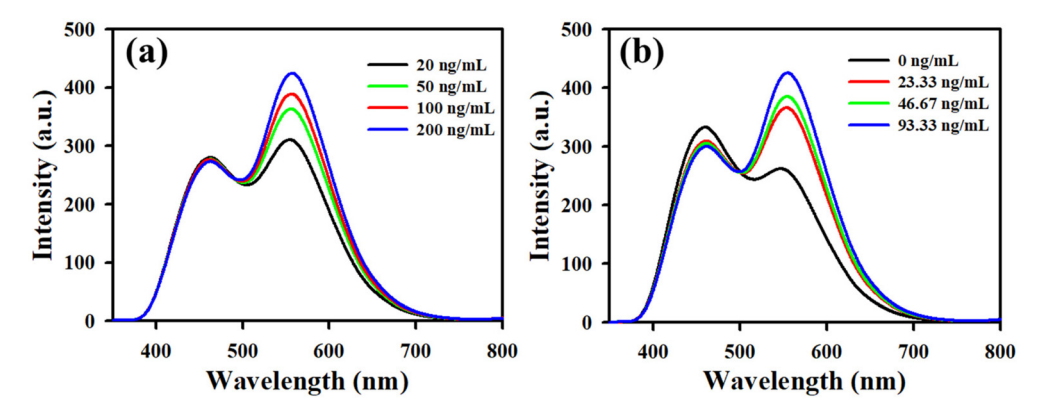


Fig. 6 (a) Fluorescence spectra of the system with varied concentrations of acephate spiked in tap water (20, 50, 100 and 200 ng mL⁻¹). (b) Fluorescence spectra of the system with varied concentrations of acephate spiked in pear (0, 23.33, 46.67, and 93.33 ng mL⁻¹).

Table 2 Determination of acephate in tap water samples

Sample	Added value (ng mL ⁻¹)	Found (ng mL ⁻¹)	Recovery $(n = 3, \%)$	RSD (n = 3, %)
Tap water	0	_	_	_
	20	21.33	106.65	1.28
	50	47.89	95.78	1.03
	100	106.09	106.09	0.98
	200	202.30	101.15	1.17

Tap water was spiked with different concentrations of acephate (20, 50, 100 and 200 ng mL⁻¹) using the standard addition method. Fig. 6(a) shows the fluorescence spectrum under 360 nm excitation after adding 20, 50, 100, and 200 ng mL⁻¹ acephate to tap water. To study the accuracy of the detection system, we conducted a recovery test using the standard addition method. As shown in Table 2, the recovery rates of acephate for known spiked samples were measured in the range of 95–106.65% for tap water samples, and a relative standard deviation (RSD) of less than 1.28% was obtained, indicating the good accuracy and high reproducibility of our method.

The method was further validated by testing pear samples. The pear samples were prepared according to the "Real sample preparation" section, in which the spiked concentrations were 0, 23.33, 46.67, 70.00, and 93.33 ng mL⁻¹. Fig. 6(b) shows the fluorescence spectra of pear samples spiked with different concentrations of acephate. As listed in Table 3, the recoveries for the pear samples spiked with known concentrations of acephate were determined to be in the range of 93.51–111.15%,

Table 3 Determination results of acephate in pear samples

Sample	Added value (ng mL ⁻¹)	Found (ng mL ⁻¹)	Recovery $(n = 3, \%)$	RSD (n = 3, %)
Pear 0 23.33 46.67 93.33	0	_	_	_
	23.33	25.93	111.15	4.17
	46.67	43.64	93.51	3.87
	93.33	98.60	105.64	4.23

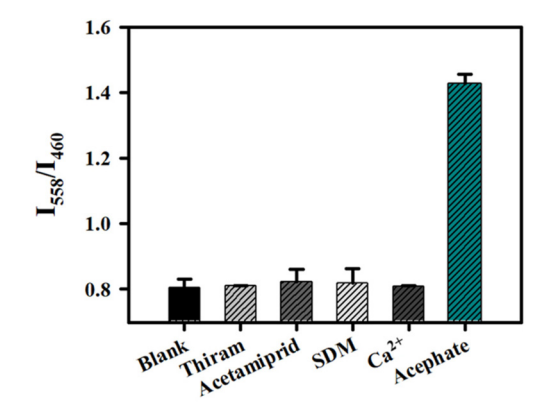


Fig. 7 Selectivity investigation. Acephate, 100 $\,\mathrm{ng}\,\,\mathrm{mL}^{-1}$; other interfering agents, 1000 $\,\mathrm{ng}\,\,\mathrm{mL}^{-1}$.

which met the criterion of quality control of laboratory-chemical testing of food.

3.6 Selectivity of the detection system

To evaluate the selectivity of the detection system, other interfering substances (acetamiprid, thiram, sulfa antibiotics (SDM), and $\mathrm{Ca^{2^+}}$) at 1000 ng mL⁻¹ were chosen to investigate the anti-interference ability of our method, while the concentration of acephate was kept at 100 ng mL⁻¹. As shown in Fig. 7, the signal intensity ratio I_{558}/I_{460} of acephate was the highest, reaching 1.43, whereas the ratiometric signals I_{558}/I_{460} of the other interfering substances were similar to that of the blank and much lower than the signal caused by acephate, even though high concentrations of interfering substances were used. These results indicated that the detection system has high selectivity for organophosphorus pesticides.

4. Conclusion

In summary, a new enzyme inhibition method combined with the IFE effect has been developed for the sensitive quantitative detection of acephate. The dual effects from the CQD-emitted Paper Analyst

fluorescence and the inhibitory effect from DAP (*i.e.*, IFE), which was correlated to the concentration of OPs, produce the ratiometric fluorescence response, which was used for the quantitative detection of OPs. The detection limit of this method is 0.052 ppb, which is far lower than the standards for acephate from China and EU in food safety administration (*e.g.*, 0.02 ppm for China). Compared with traditional enzyme inhibition methods, this method exhibits much higher detection sensitivity. Leveraging a portable fluorescence detector and an integrated microfluidic device to be developed, ^{35–38} this method will have great potential for rapid and ultrasensitive screening of trace pesticide residues on site, and broad application in food safety testing, environmental pollution monitoring, and poisoning estimation.

Author contributions

Haiqin Li: conceptualization, methodology, formal analysis, investigation, validation, data curation, writing – original draft, writing – review and editing. Rong Deng: conceptualization, methodology, formal analysis. Hamed Tavakoli: writing – review and editing. Xiaochun Li: project administration, conceptualization, formal analysis, supervision, funding acquisition, methodology, resources, writing – review and editing. XiuJun Li: formal analysis, conceptualization, methodology, resources, writing – review and editing.

Conflicts of interest

The authors declare the following competing financial interest (s). The authors from TYUT have filed a China Patent Application (No. 202110392652. 4) to protect the IP associated with the technology described in this paper. Other authors declare no competing interest.

Acknowledgements

We gratefully acknowledge the financial support from the National Natural Science Foundation of China (grant no. 21874098), Shanxi Province International Collaboration Project (grant no. 201903D421053), and University Scientific and Technological Transformation and Cultivation Project of Shanxi province. We are also grateful to the support from the U.S. CPRIT (RP210165), the U.S. NSF (IIP2122712, IIP2052347, and CHE2216473), the NIH/NIAID (R41AI162477), and the U.S. DOT (CARTEEH).

References

S. V. Boxstael, I. Habib, L. Jacxsens, M. D. Vocht, L. Baert,
 E. V. de Perre, A. Rajkovic, F. Lopez-Galvez, I. Sampers,
 P. Spanoghe, B. D. Meulenaer and M. Uyttendaele, Food safety issues in fresh produce: bacterial pathogens, viruses and pesticide residues indicated as major concerns by sta-

keholders in the fresh produce chain, *Food Control*, 2013, 32, 190–197.

- 2 G. T. Bakirci, D. B. Y. Acay, F. Bakirci and S. Otles, Pesticide residues in fruits and vegetables from the Aegean region, Turkey, *Food Chem.*, 2014, **160**, 379–392.
- 3 L. Wan, Y. Wu, H. Ding and W. Zhang, Toxicity, Biodegradation, and Metabolic Fate of Organophosphorus Pesticide Trichlorfon on the Freshwater Algae Chlamydomonas reinhardtii, *J. Agric. Food Chem.*, 2020, **68**, 1645–1653.
- 4 J. R. Richardson, H. W. Chambers and J. E. Chambers, Analysis of the additivity of in vitro inhibition of cholinesterase by mixtures of chlorpyrifos-oxon and azinphosmethyl-oxon, *Toxicol. Appl. Pharmacol.*, 2001, 172, 128–139.
- 5 M. Eddleston, N. A. Buckley, P. Eyer and A. H. Dawson, Management of acute organophosphorus pesticide poisoning, *Lancet*, 2008, 371, 597–607.
- 6 https://www.who.int/news-room/fact-sheets/detail/pesticide-residues-in-food.
- 7 C. R. Bojaca, L. A. Arias, D. A. Ahumada, H. A. Casilimas and E. Schrevens, Evaluation of pesticide residues in open field and greenhouse tomatoes from Colombia, *Food Control*, 2013, 30, 400–403.
- 8 P. Pugliese, J. C. Moltó, P. Damiani, R. Marín, L. Cossignani and J. Manes, Gas chromatographic evaluation of pesticide residue contents in nectarines after non-toxic washing treatments, *J. Chromatogr. A*, 2004, **1050**, 185–191.
- 9 X. Mao, A. Yan, Y. Wan, D. Luo and H. Yang, Dispersive Solid-Phase Extraction Using Microporous Sorbent UiO-66 Coupled to Gas Chromatography-Tandem Mass Spectrometry: A QuEChERS-Type Method for the Determination of Organophosphorus Pesticide Residues in Edible Vegetable Oils without Matrix Interference, *J. Agric. Food Chem.*, 2019, 67, 1760–1770.
- 10 K. Seebunrueng, Y. Santaladchaiyakit and S. Srijaranai, Vortex-assisted low-density solvent based demulsified dispersive liquid-liquid microextraction and high-performance liquid chromatography for the determination of OP in water samples, *Chemosphere*, 2014, 103, 51–58.
- 11 C. García-Ruiz, G. Álvarez-Llamas, Á. Puerta, E. Blanco, A. Sanz-Medel and M. Marina, Enantiomeric separation of OP by capillary electrophoresis: Application to the determination of malathion in water samples after preconcentration by off-line solid-phase extraction, *Anal. Chim. Acta*, 2005, 543, 77–83.
- 12 J. Yao, Z. Wang, L. Guo, X. Xu, L. Liu, L. Xu, S. Song, C. Xu and H. Kuang, Advances in immunoassays for organophosphorus and pyrethroid pesticides, *TrAC, Trends Anal. Chem.*, 2020, **131**, 116022.
- 13 F. Arduinia, S. Cinti, V. Caratelli, L. Amendola, G. Palleschi and D. Moscone, Origami multiple paper-based electrochemical biosensors for pesticide detection, *Biosens. Bioelectron.*, 2019, **126**, 346–354.
- 14 X. Xie, B. Zhou, Y. Zhang, G. Zhao and B. Zhao, A multi-residue electrochemical biosensor based on graphene/chitosan/parathion for sensitive OP detection, *Chem. Phys. Lett.*, 2021, **767**, 138355.

15 J. Guo, J. X. H. Wong, C. Cui, X. Li and H.-Z. Yu, A smart-phone-readable barcode assay for the detection and quantitation of pesticide residues, *Analyst*, 2015, **140**, 5518–5525.

- 16 X. Meng, C. W. Schultz, C. Cui, X. Li and H.-Z. Yua, On-site chip-based colorimetric quantitation of OP using an office scanner, *Sens. Actuators*, *B*, 2015, 215, 577–583.
- 17 I. Jang, D. B. Carrão, R. F. Menger, A. R. M. de Oliveira and C. S. Henry, Pump-Free microfluidic rapid mixer combined with a paper-based channel, *ACS Sens.*, 2020, 5, 2230–2238.
- 18 A. V. Alex and A. Mukherjee, Review of recent developments (2018–2020) on ATChsterase inhibition-based biosensors for OP detection, *Microchem. J.*, 2021, **161**, 105779.
- 19 M. Zhang, J. Yang, Y. Wang, H. Sun, H. Zhou, X. Liu, C. Ye, Z. Bao, J. Liu and Y. Wu, Plasmon-coupled 3D porous hotspot architecture for super-sensitive quantitative SERS sensing of toxic substances on real sample surfaces, *Phys. Chem. Chem. Phys.*, 2019, 21, 19288–19297.
- 20 S. Weng, W. Zhu, P. Li, H. Yuan, X. Zhang, L. Zheng, J. Zhao, L. Huang and P. Han, Dynamic surface-enhanced Raman spectroscopy for the detection of acephate residue in rice by using gold nanorods modified with cysteamine and multivariant methods, *Food Chem.*, 2020, **310**, 125855.
- 21 H. Tavakoli, W. Zhou, L. Ma, S. Perez, A. Ibarra, F. Xu, S. Zhan and X. Li, Recent advances in microfluidic platforms for single-cell analysis in cancer biology, diagnosis and therapy, *TrAC*, *Trends Anal. Chem.*, 2019, 117, 13–26.
- 22 M. Lv, W. Zhou, H. Tavakoli, C. Bautista, J. Xia, Z. Wang and X. Li, Aptamer-functionalized Metal-organic frameworks (MOFs) for biosensing, *Biosens. Bioelectron.*, 2021, 176, 112947.
- 23 R. Jin, D. Kong, X. Yan, X. Zhao, H. Li, F. Liu, P. Sun, Y. Lin and G. Lu, Integrating Target-Responsive Hydrogels with Smartphone for On-Site ppb-Level Quantitation of Organophosphate Pesticides, *ACS Appl. Mater. Interfaces*, 2019, **11**, 27605–27614.
- 24 Q. Wang, Q. Yin, Y. Fan, L. Zhang, Y. Xu, O. Hu, X. Guo, Q. Shi, H. Fu and Y. She, Double quantum dots-nanoporphyrin fluorescence-visualized paper-based sensors for detecting OP, *Talanta*, 2019, **199**, 46–53.
- 25 M. Jiang, C. Chen, J. He, H. Zhang and Z. Xu, Fluorescence assay for three OP in agricultural products based on Magnetic-Assisted fluorescence labeling aptamer probe, Food Chem., 2020, 307, 125534.
- 26 J. Wang, J. Zhang, J. Wang, G. Fang, J. Liu and S. Wang, Fluorescent peptide probes for organophosphorus pesticides detection, *J. Hazard. Mater.*, 2020, **389**, 122074.

- 27 S. Zhu, Q. Meng, L. Wang, J. Zhang, Y. Song, H. Jin, K. Zhang, H. Sun, H. Wang and B. Yang, Highly photoluminescent carbon dots for multicolor patterning, sensors, and bioimaging, *Angew. Chem., Int. Ed.*, 2013, 52, 3953– 3957.
- 28 S. Y. Lim, W. Shen and Z. Gao, Carbon quantum dots and their applications, *Chem. Soc. Rev.*, 2015, 44, 362–381.
- 29 S. Lu, G. Li, Z. Lv, N. Qiu, W. Kong, P. Gong, G. Chen, L. Xia, X. Guo, J. You and Y. Wu, Facile and ultrasensitive fluorescence sensor platform for tumor invasive biomaker beta-glucuronidase detection and inhibitor evaluation with carbon quantum dots based on inner-filter effect, *Biosens. Bioelectron.*, 2016, 85, 358–362.
- 30 X. Li, S. Zhao, B. Li, K. Yang, M. Lan and L. Zeng, Advances and perspectives in carbon dot-based fluorescent probes: Mechanism, and application, *Coord. Chem. Rev.*, 2021, 431, 213686.
- 31 J. Wang, Q. Liu, Y. Liang and G. Jiang, Recent progress in application of carbon nanomaterials in laser desorption/ionization mass spectrometry, *Anal. Bioanal. Chem.*, 2016, 408, 2861–2873.
- 32 B. G. Katzung, *Basic and clinical pharmacology:Introduction to autonomic pharmacology*, The McGraw Hill Companies, 8 edn, 2001, pp. 75–91. ISBN: 978-0-07-160405-5.
- 33 J. Zhang, W. Zheng and X. Jiang, Ag+ -Gated Surface Chemistry of Gold Nanoparticles and Colorimetric Detection of Acetylcholinesterase, *Small*, 2018, **14**, 1801680.
- 34 X. Zhao, W. N. Kong, J. Wei and M. Yang, Gas chromatography with flame photometric detection of 31organophosphorus pesticide residues in Alpinia oxyphylla dried fruits, *Food Chem.*, 2014, **162**, 270–276.
- 35 W. Zhou, M. Dou, S. S. Timilsina, F. Xu and X. Li, Recent innovations in cost-effective polymer and paper hybrid microfluidic devices, *Lab Chip*, 2021, 21, 2658–2683.
- 36 M. Dou, S. T. Sanjay, M. Benhabib, F. Xu and X. Li, Lowcost Bioanalysis on Paper-based & Its Hybrid Microfluidic Platforms, *Talanta*, 2015, **145**, 43–54.
- 37 M. Dou, N. Macias, F. Shen, J. D. Bard, D. C. Domínguez and X. Li, Rapid and Accurate Diagnosis of the Respiratory Disease Pertussis on a Point-of-Care Biochip, *EClin. Med.*, 2019, **8**, 72–77.
- 38 K. S. Prasad, X. Cao, N. Gao, Q. Jin, S. T. Sanjay, G. Henao-Pabon and X. Li, A Low-Cost Nanomaterial-based Electrochemical Immunosensor on Paper for High-sensitivity Early Detection of Pancreatic Cancer, *Sens. Actuators, B*, 2020, **305**, 127516.